

**THREE-DIMENSIONAL SHAPES AND IMPACTOR SIZE ESTIMATION OF STARDUST IMPACT TRACKS.** Y. Iida<sup>1</sup>, A. Tsuchiyama<sup>1</sup>, T. Kadono<sup>2</sup>, T. Nakamura<sup>3</sup>, K. Sakamoto<sup>3</sup>, T. Nakano<sup>4</sup>, K. Uesugi<sup>5</sup>, and M. E. Zolensky<sup>6</sup>, <sup>1</sup>Department of Earth and Space Science, Graduate School of Science, Osaka University, Toyonaka 560-0043, Japan, Japan ([iida@ess.sci.osaka-u.ac.jp](mailto:iida@ess.sci.osaka-u.ac.jp), [akira@ess.sci.osaka-u.ac.jp](mailto:akira@ess.sci.osaka-u.ac.jp)), <sup>2</sup>Institute of Laser Engineering, Osaka University, Suita 565-0871, Japan, <sup>3</sup>Department of Earth and Planetary Science, Faculty of Science, Kyushu University, Hakozaki, Fukuoka 812-8581, Japan, <sup>4</sup>Geological Survey of Japan, Advanced Industrial Science and Technology, Tsukuba 305-8567, Japan, <sup>5</sup>Synchrotron Radiation Research Institute, SPring-8, Sayo, Hyogo 679-5198, Japan, <sup>6</sup>KT NASA Johnson Space Center Houston, TX 77058, USA.

**Introduction:** Impact tracks formed by cometary dust capture in silica aerogel collectors in the Stardust mission [1] have a variety of shapes, showing diversity of the cometary dust [2]. We have investigated 3-D structures and elemental distributions of three impact tracks using synchrotron radiation x-ray analyses (microtomography and XRF) as one of the preliminary examination [3]. In this study, additional five tracks were investigated by the same analytical method. Impactor sizes of the tracks were estimated from the track entrance sizes and Fe abundances. Size parameters, such as length, of the tracks were normalized by the impactor size to compare track shapes.

**Experiments:** In addition to the previous three tracks (T46 *Gobou* (carrot,  $\approx 930 \mu\text{m}$ ), T67 *Namekuji* (bulbous,  $120 \mu\text{m}$ ), and T68 *Skyrocket* (carrot,  $2690 \mu\text{m}$ )), five impact track were investigated: T96 *Ichiro* (carrot,  $660 \mu\text{m}$ ), T97 (carrot,  $650 \mu\text{m}$ ), T98 *Heiji* (cylinder,  $1910 \mu\text{m}$ ), T99 *Spiral-B* (carrot, spiral shaped,  $6250 \mu\text{m}$ ), and T100 *Spiral-A* (carrot, spiral shaped,  $8320 \mu\text{m}$ ).

Keystones having these impact tracks were analyzed at beamline BL47XU of SPring-8, Japan. Three-dimensional structures of the tracks were obtained by projection microtomography [4] at 8-10 keV with 1500-3600 projections for each slice. The voxel (pixel in 3-D) size was  $0.21 \times 0.21 \times 0.21$ ,  $0.50 \times 0.50 \times 0.50$  or  $1.05 \times 1.05 \times 1.05 \mu\text{m}^3$  depending on the track size. XRF analysis was performed at 15 keV using a Ge-SSD to determine the elemental abundances (mainly Fe) along the track and individual grains.

**CT image analysis:** Track cavities including radial cracks, condensed aerogels and captured grains including terminal grains were recognized in CT images, and external shapes of the tracks based on the above features were obtained as digital images (Fig.1). Quantitative sizes parameters of the track, such as length, were obtained based on the voxel size of the CT images. By assuming cylindrical symmetry of the tracks, we also calculated quantitative track shape. *i.e.*,

track diameter,  $D$ , as a function of track depth,  $Z$  (Fig.2). At the track entrance,  $D$  decrease first and then increases with increasing  $Z$ . Track entrance size,  $D_e$ , was determined as the minimum diameter.

#### Results and Discussion:

**Track morphologies.** T96 (*Ichiro*) has relatively large cavity close to the terminal grain. Thus, the track looks like a baseball bat (Fig.1d). The terminal grain is smaller than the cavity although we do not know this reason at present. T97 is bifurcated into two thin tracks with a relatively large subtrack (Fig.1e). T98 (*Heiji*) is a cylinder-type track and bifurcated into two thin tracks (Fig.1f). It looks like “jitte”, one of an old Japanese weapon.

T99 and T100 (*Spiral-A* and *-B*) are present close together ( $\sim 700 \mu\text{m}$  apart). Both tracks look like a spiral in shape under an optical microscope. This spiral feature is caused by radial cracks spirally developing from the track wall outwards (Fig.1gh). However, the spiral cracks cover only a half side of the wall. The spiral signs of the both tracks are the same (anti-clockwise from the entrance to the end). The spiral feature might be explained by spinning of impactors with a shape of screw propeller or local strain in aerogel with a spiral symmetry.

**Impactor size estimation.** The entrance size of a hypervelocity impact track is related to the impactor size [5]. However, it is generally difficult to measure the entrance size accurately under an optical microscope. Observation by microtomography enables us to measure the accurate size,  $D_e$  (Fig.2).

The impactor size can be also estimated from the Fe content of the track, that is the Fe content of the impactor,  $m(\text{Fe})_p$ . In the XRF measurement, the mass can be obtained by  $m(\text{Fe})_p = C(\text{Fe})/[S(\text{Si})F]$ , where  $C(\text{Fe})$  is the x-ray count rates of Fe throughout a track, and  $S(\text{Si})$  is Si sensitivity determined by measurements of clear aerogel.  $F$  is the ratio of the sensitivities of Fe and Si ( $F = S(\text{Fe})/S(\text{Si})$ ) and treated as a parameter in this study as we do not know the exact value of  $F$  at

present. The value is estimated to be the order of 10-100 based on the Fe-K and Si-K fluorescence yields and x-ray absorptions, and will be determined near future. In this paper, the impactor size,  $D_p$ , was estimated with the parameter  $F$  by assuming the Fe content of CI composition (18.67 wt.%) and densities of fine aggregate ( $1 \text{ g/cm}^3$ ) and crystalline particle ( $3 \text{ g/cm}^3$ ).

Figure 3 shows the comparison between  $D_e$  and  $F^{1/3}D_p$ . As the Fe abundances of the terminal grains of T46 (*Gobou*) and T100 (*Spiral-A*) were not determined,  $F^{1/3}D_p$  of these tracks are the lower limits. T98 (*Heiji*) has a large amount of Fe compared with  $D_e$  and the track size (e.g.,  $L_t$ ) as well, and the impactor of this track might be mainly metallic iron and/or iron sulfides. The correlation for the other tracks are good;  $F^{1/3}D_p = 1.67(\pm 0.11) \times D_e$ . We can estimate  $F^{1/3}D_p$  by using this equation from  $D_e$  if the Fe content is not known.

*Track shapes normalized by the impactor size.* The track shapes were normalized by the impactor size for comparison between tracks (Fig.4). The  $D/[F^{1/3}D_p] - Z/[F^{1/3}D_p]$  curves are almost the same for the carrot-type tracks, which have bulbous portions near the entrances and thin tracks (T46, T68, T96, T97, T99 and T100). The bulbous portion of T67 (*Namekuji*) is wider and the cylinder-type T98 (*Heiji*) is longer than the carrot-type tracks. The similarity of the normalized shapes suggests that the impactors of these tracks are almost similar irrespective of their sizes because the other impact conditions, such as impact velocity and aerogel density, are the same.

**References:** [1] Brownlee D. et al. (2006) *Science*, 314, 1711. [2] Hörzt F. et al. (2006) *Science*, 314, 1716. [3] Tsuchiyama et al. *MAPS*, submitted. [4] Uesugi et al. (2003) *Journal de Physique. IV France*, 104, 45. [5] Burchell et al., (1999) *Planet. Space Sci.*, 47, 189. [6] Nakamura et al. (2007) *MAPS*, in press.

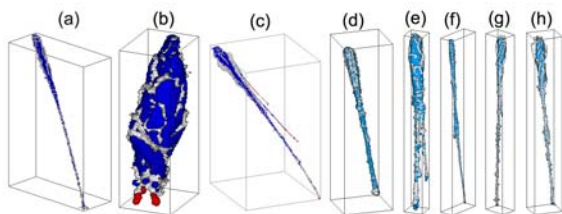


Figure 1. Bird's eye views of the impact tracks obtained by microtomography. Gray: track cavity including radial cracks. (a) T46 (*Gobou*)  $\geq 930 \mu\text{m}$ , (b) T67 (*Namekuji*)  $120 \mu\text{m}$ , (c) T68 (*Skyrocket*)  $2690 \mu\text{m}$ , (d) T96 (*Ichiro*)  $660 \mu\text{m}$ , (e) T97  $650 \mu\text{m}$ , (f) T98 (*Heiji*)  $1910 \mu\text{m}$ , (g) T99 (*Spiral-B*)  $6250 \mu\text{m}$ , (h) T100 (*Spiral-A*)  $8320 \mu\text{m}$ .

$\mu\text{m}$ , (h) T100 (*Spiral-A*)  $8320 \mu\text{m}$ . Blue (Cyan): condensed (melted and/or compressed) aerogel. Red: captured grains (most of them are mixtures of fine grained dust and melted aerogel [6]).

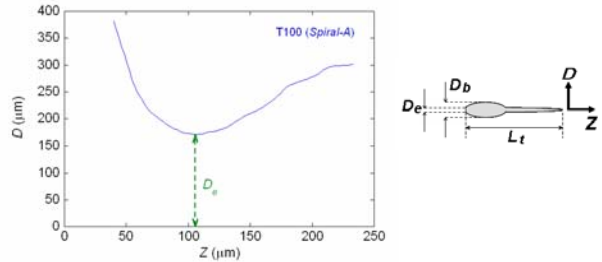


Figure 2. Track diameter,  $D$ , as a function of the track depth,  $Z$ , at the entrance of T100 (*Spiral-A*). The track entrance size,  $D_e$ , was determined as the minimum diameter. See also Fig.4 for the whole track.

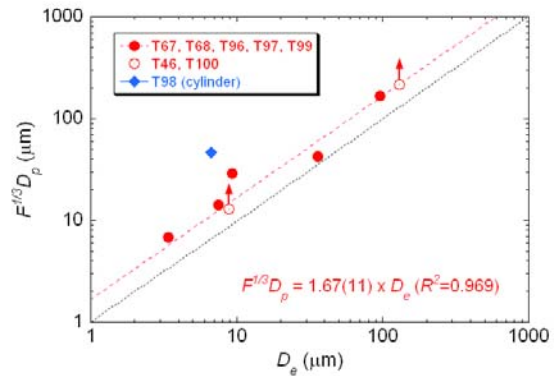


Figure 3. Relation between track entrance size,  $D_e$ , and impactor size,  $D_p$ , estimated from the track Fe abundance.  $F$  is the ratio of the sensitivities of Fe and Si ( $F^{1/3} \sim 2-5$ ).

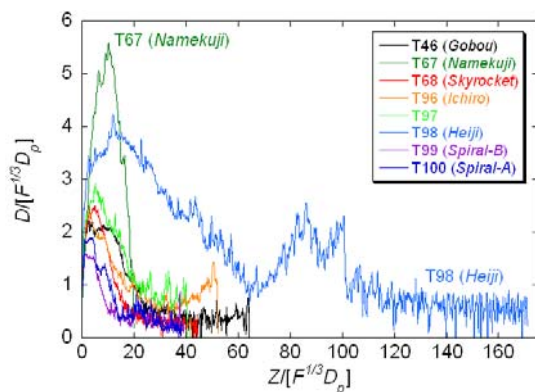


Figure 4. Track shapes normalized by the impactor size,  $D_p$ , with the ratio of the sensitivities of Fe and Si,  $F$  ( $F^{1/3} \sim 2-5$ ).